Estimation of Sounding Uncertainty from Measurements of Water Mass Variability

By Jonathan Beaudoin [1], B. Calder [2], J. Hiebert [3] and G. Imahori [4], Canada

Abstract

Analysis techniques are introduced that allow for estimation of potential sounding uncertainty due to water mass variability from reconnaissance campaigns in which oceanographic parameters are measured at a high temporal and spatial resolution. The analysis techniques do not require sounding data, thus analyses can be tailored to match any survey system; this allows for pre-analysis campaigns to optimize survey instrumentation and sound speed profiling rates such that a desired survey specification can be maintained. Additionally, the output of the analysis methods can potentially provide a higher fidelity estimation of sounding uncertainty due to water mass variability than uncertainty models in common use.

Résumé

Des techniques d'analyse sont introduites afin de permettre l'estimation de l'incertitude potentielle des sondes due à la variabilité de la masse d'eau à partir de campagnes de reconnaissance dans lesquelles les paramètres océanographiques sont mesurés avec une haute résolution temporelle et spatiale. Les techniques d'analyse ne nécessitant pas de données de sondes, les analyses peuvent donc être ajustées pour s'adapter à tout système de levés ; ceci permet aux campagnes de pré-analyse d'optimiser l'instrumentation hydrographique ainsi que les niveaux de profilage de la vitesse du son de manière à conserver une spécification de levé souhaitée. En outre, le résultat des méthodes d'analyse peut potentiellement fournir une estimation à plus haute fidélité, en ce qui concerne les incertitudes des sondes du fait de la variabilité de la masse d'eau, que les modèles d'incertitude en usage.

Resumen

Se presentan análisis técnicos que permiten una estimación de posibles incertidumbres en los sondeos, debidas a la variabilidad de la masa de agua, procedentes de campañas de reconocimiento en las que los parámetros oceanográficos son medidos con una resolución temporal y espacial elevada. Los análisis técnicos no requieren los datos de sondeos, así pues dichos análisis pueden adaptarse a cualquier sistema hidrográfico. Esto permite campañas de análisis previos para optimizar la instrumentación hidrográfica y los niveles de descripción de la velocidad del sonido, para que pueda mantenerse una especificación hidrográfica deseada. Además, el resultado de los métodos analíticos puede proporcionar potencialmente una estimación de la fidelidad de las incertidumbres en los sondeos, debidas a una variabilidad de la masa de agua mayor que la de los modelos de incertidumbres que se utilizan corrientemente.

[1] Ocean Mapping Group, University of New Brunswick, Fredericton, NB, Canada
[2] Center for Coastal and Ocean Mapping and NOAA-UNH Joint Hydrographic Center, University of New Hampshire, Durham, NH, USA
[3] NOAA Hydrographic Systems and Technology Program, Silver Spring, MB, USA
[4] NOAA Office of Coast Survey, Silver Spring, MD, USA

1.   Introduction

Multibeam echosounders (MBES) collect oblique soundings, allowing for a remarkable increase in coverage compared to traditional downward looking single beam echosounders (SBES). The gain in coverage comes at a cost: the speed of sound varies with depth and can cause the oblique sounding ray paths to bend, introducing significant and systematic biases in soundings. This is readily corrected by measuring the sound speed variation with depth and using this additional information to model the acoustic ray path. Underway sound speed profiling instrumentation has been used to measure sound speed profiles at a high rate since the late 1990s (Furlong et al., 1997) providing hydrographers with an unprecedented ability to sample the oceanographic environment through which they sample the seafloor. *Figure 1* provides an example of sound speed casts collected with underway instrumentation.
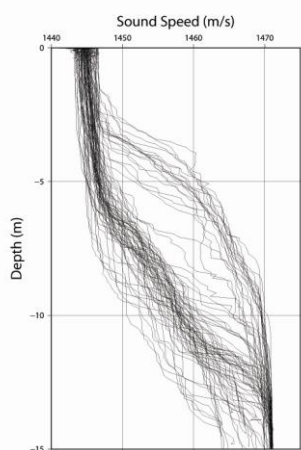
Figure 1: Plot of 82 sound speed casts gathered over a 2.5 hour interval near the mouth of the Rotterdam Waterway in March 2009

Though such tools provide ample data to the hydrographer, it has been difficult to extract meaningful information regarding the impact of water column variability on sounding uncertainty. Previous work has dealt with integrating near-continuous sound speed information into the data processing stream and assessing the impact of insufficient water column sampling in areas of dynamic oceanography through sounding by sounding comparison before and after ray tracing correction (Hughes Clarke et al., 2000). Other work has used the differencing of digital terrain models derived from soundings to ascertain the impact of using oceanographic models in the place of sound speed observations (Calder et al., 2004).

These techniques have several drawbacks. Firstly, they require the use of sounding data; thus one must sample the seafloor in order to learn about the sea. Secondly, as the methods require soundings, the findings from such analyses are only applicable to the sounding geometry with which the seafloor was mapped and it is difficult to extrapolate from the findings to ascertain how other sounding geometries might react to the same oceanographic conditions. Thirdly, post-processing of sounding data is required, which can involve significant operator interaction and time, thus these techniques are not well suited to timely evaluations of water mass variability.

In this work we propose a numerical simulation method which can be used to assess the impact of water column variability on sounding uncertainty without any requirement for soundings, i.e. sound speed casts are the sole required input. The simulation works by mimicking the ray tracing portion of the MBES depth reduction procedure and can be configured to match the sounding geometry of any MBES system. The simulator also investigates the entire potential sounding space, i.e. from sounder to seafloor and across the entire angular sector, generating what we refer to as an "uncertainty wedge" (Beaudoin, 2008). Analysis methods are shown that can (a) quantify the impact of observed variability in terms of sounding uncertainty, and (b) analyze sounding uncertainties associated with various sampling regimes, e.g. sampling every few minutes versus every few hours. As the simulator requires no sounding data and can generate results in near real-time, it is ideally paired with underway sound speed instrumentation where the combination of sensor and simulation software provides the hydrographer with a potent rapid environmental assessment (REA) tool.

Fundamentals of uncertainty wedge calculation and analysis are discussed in the next section, followed by examination of sample problems which demonstrate the application of uncertainty wedge analysis techniques to common types of problems in hydrographic surveying. Finally, the issue of integrating uncertainty wedges (and the analysis techniques described herein) into existing algorithms and workflows is discussed.

2.   Method

The simulator is based upon monitoring the progression of two or more acoustic ray paths, all sharing a common initial launch, or depression,

angle and each ray path being associated with a particular sound speed profile. Variable parameters include draft, angular sector, range performance envelope, and the use of a surface sound speed probe measurement to augment the ray tracing algorithm (though surface sound speed probe data are not required). Appendix A discusses the case of simulating the inclusion of a surface sound speed measurement. In the numerical simulation, a constant velocity acoustic ray tracing algorithm (Medwin and Clay, 1998) is used to explore how differing measurements of the sound speed structure, e.g. the two sound speed profiles shown in *Figure 2,* can alter the ray path, and ultimately, the divergence of the set

of ray traced solutions for a given two-way travel-time (TWTT) and depression angle, as shown in *Figure 3*. By systematically modifying the depression angle and TWTT, the entire potential sounding space is explored to populate a depth and distance indexed table of sounding depth and horizontal discrepancies, as shown in *Figures 4 and 5*. In these figures, the sounder would be situated at the apex of the wedge on the upper left. The wedge shaped look-up table represents half of the angular sector covered by the mapping system and uncertainty is assumed to be symmetric about the vertical axis. These tables are referred to as uncertainty wedges throughout the remainder of this work.
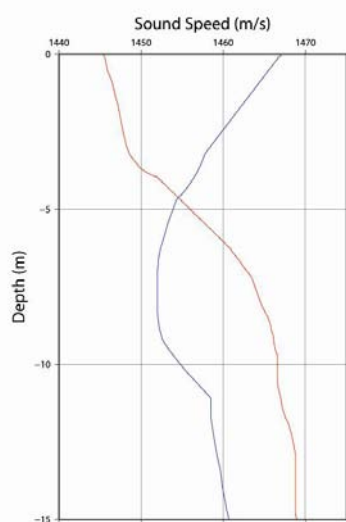
Figure 2: Two sample sound speed profiles
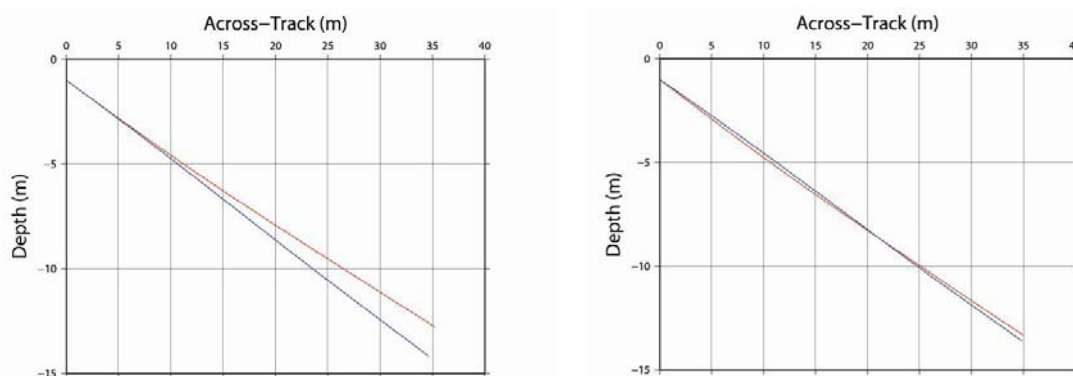
Figure 3: Ray trace solutions associated with sound speed casts in Figure 2; the simulated draft is 1.0 m, depression angle is 20° and TWTT is 0.051 s. The ray traces in Panel A demonstrate how dramatic variations in the water column can cause great divergence in the ray paths. Panel B demonstrates how using a surface sound speed probe has the potential to mitigate the effects of surface variability in some cases. In this latter case, the solutions were computed using a common surface sound speed value of 1455 m s⁻¹.
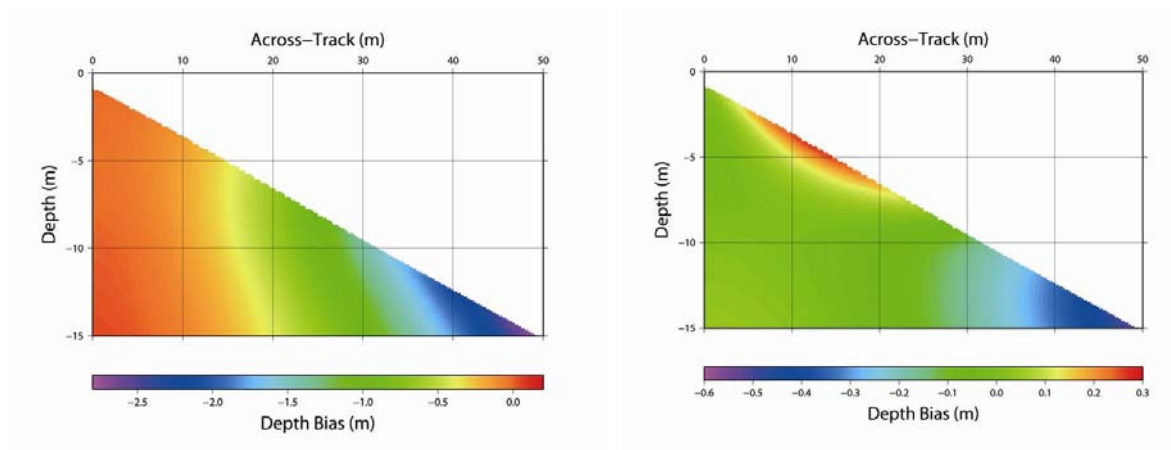
Figure 4: Depth uncertainty wedges associated with casts in Figure 2; simulated draft is 1.0 m and angular sector is 150°. As in Figure 3, Panel A and B show the cases of independent and common surface sound speeds, respectively. Note the different colour scales for each panel.
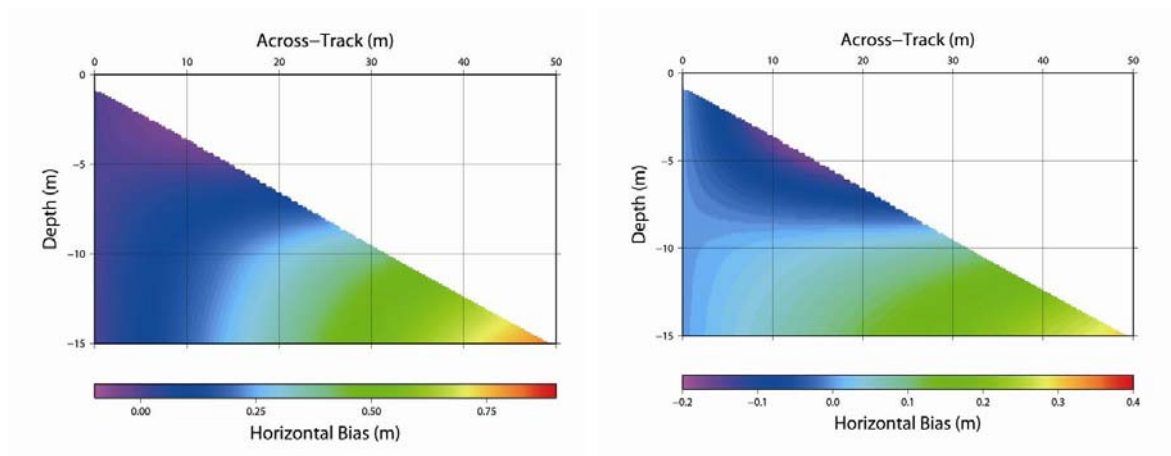
Figure 5: Horizontal uncertainty wedges associated with casts in Figure 2; simulated draft is 1.0 m and angular sector is 150°. As in Figure 3, Panel A and B show the cases of independent and common surface sound speeds, respectively. Note the different colour scales for each panel.
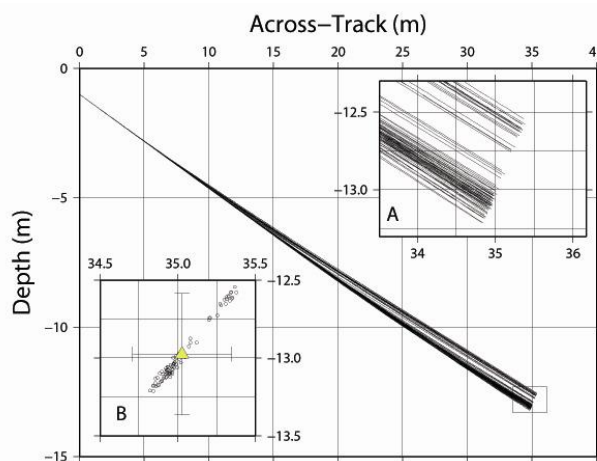
Figure 6: Ray paths calculated for the 82 sound speed profiles shown in Figure 1 using a draft of 1.0 m, a depression angle of 20°, a TWTT of 0.051 s and a common surface sound speed of 1445 m s^{-1}. The inset panel (A) on the upper right corresponds to the rectangular box drawn near the termini of the ray paths shown in the main panel. The lower left panel (B) shows the ends of the ray paths only and demonstrates how the final ray traced solutions disperse depending on which sound speed profile is used for ray tracing. The mean depth and position are indicated by the yellow triangle, the error bars indicate the 95% confidence level. Note that the main panel and upper right panel share the same distorted aspect ratio whereas the aspect ratio of the lower left panel is correct.

Though one could constrain the analysis to the nominal seafloor depth, we have chosen to investigate the entire potential sounding space for two reasons. Firstly, the seafloor is not always flat and it is sometimes necessary to estimate the effect of refraction based uncertainties for depths shoaller than the nominal seafloor depth. An extreme example is the mast of a shipwreck that is safely above the depth of variability (or vice versa). Secondly, it is important to understand at what depth the divergence in ray paths occurs for REA and/or planning purposes, as will be demonstrated later in Section 3.2.

The ray trace simulator can be used to track the dispersion of ray paths associated with a set of several sound speed profiles representing a sample of the population of possible water column conditions in a given area. This type of analysis, referred to as a Variability Analysis (VA), allows for the construction of a variability wedge, or a v-wedge, which quantifies the "potential uncertainty" associated with water mass variability. *Figure 6* demonstrates the principle behind the estimation of the potential horizontal and depth uncertainty for a single location in the potential sounding space. The uncertainty associated with observed water mass variability is estimated as the standard deviation computed from the terminal points of a set of ray traced solutions where each ray is traced using one of the candidate sound speed profiles. The vertical and horizontal standard deviations of the set are scaled to the 95% confidence level (International Organization for Standardization-ISO, 1995) as required by most hydrographic survey order specifications. Expanding the analysis to all nodes in the sounding space, one can construct a v-wedge. For example, *Figure 7* shows a v-wedge constructed for the set of sound speed casts shown in *Figure 1*.
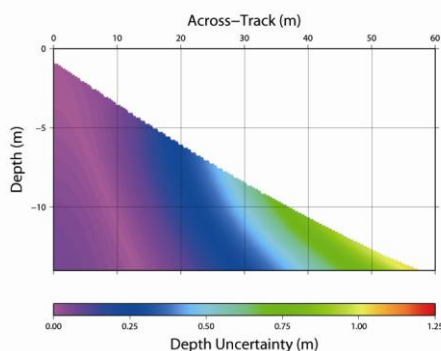
Figure 7: A Variability Wedge generated from the set of sound speed casts shown in Figure 1

An Uncertainty Wedge Analysis (UWA) consists of comparing two ray paths only, allowing for a quantitative answer to the following question: "What sounding bias would result if sound speed profile B was used in the place of sound speed profile A?", where profile A represents known conditions and profile B represents an alternate model whose fitness is to be tested by a comparison to A. As the comparison of two casts quantifies the sounding bias that would be introduced if one cast had been used in the place of the other, the resulting uncertainty wedge is more aptly named a bias wedge, or a b-wedge. By comparing many pairs of casts, a set of b-wedges can be generated; these can then be averaged to provide a mean bias wedge along with a standard deviation wedge, these being calculated for each unique position in the look-up table based on the b-wedge values at the same look-up position. The resulting mean and (appropriately scaled) standard deviation wedge are respectively referred to as an m-wedge and s-wedge in this text. In summary:

- **v-wedge (variability wedge)**: measure of the potential uncertainty associated with the spatio-temporal variability of the water column.
- **b-wedge (bias wedge)**: measure of the bias had an alternative cast been used in place of an observed cast.
- **m-wedge (mean bias wedge)**: arithmetic mean of several b-wedges.
- **s-wedge (sigma wedge)**: standard deviation associated with a set of b-wedges.

The following section demonstrates how these uncertainty representation formats and analysis techniques can be used to help the hydrographic surveyor assess the impact of water column variability on sounding accuracy.

3. Sample Analysis Problems

Time spent on reconnaissance is seldom wasted.
British Army Field Service Regulations, 1912

Much can be learned about water column variability and its impact on sounding accuracy by heavily oversampling a water mass using underway or expendable sound speed profiling instrumentation. In this section we explore how underway instrumentation and VA and UWA techniques can be used to assess the effect of water column variability, providing information that is useful for survey planning and/or execution.

3.1 Reconnaissance Data Set

A field trial was conducted by the Dutch Public Works (Rijkswaterstaat, RWS) in March of 2009 in the Rotterdam Waterway where the Meuse River meets the North Sea (see *Figure 8*) to better understand typical spatio-temporal variations in sound speed and their effect on multibeam echosounder (MBES) performance. This area was selected for the trial for two reasons. Firstly, the waterway requires frequent resurveying (13 surveys per year at 4 week intervals) due to high sedimentation rates and frequent dredging to accommodate the high volume of large draft vessel traffic. Secondly, hydrographic surveys conducted in the waterway often suffer from particularly strong refraction artifacts associated with challenging oceanographic conditions. Current survey practice is to limit survey line length to approximately 1 km, with lines parallel with the channel axis. As the channel is at most 1 km wide, a few tens of survey lines are usually required to cover any given area. The survey areas are typically easily covered in the span of a few hours with surveyors collecting a few sound speed casts over the course of the survey. Survey lines in this area are pessimistically spaced closely together to accommodate the limited ability to maintain sounding accuracy across the swath due to refraction artifacts. The overarching goal of the trial was to evaluate whether underway sampling technology such as a Moving Vessel Profiler (MVP) could address the refraction artifacts and improve survey efficiency. Given the frequent rate of resurvey and the cost in time required to survey with a pessimistic line spacing, even small gains in efficiency can have a significant cumulative benefit over time.
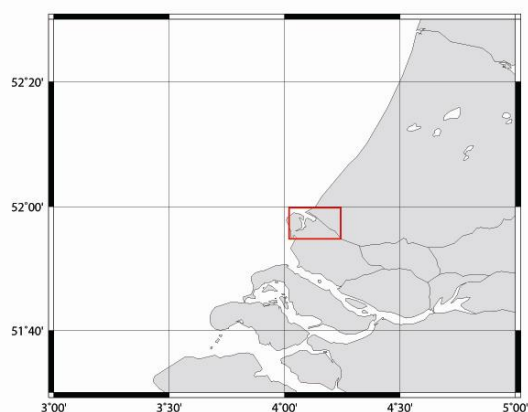
Figure 8: Overview map showing study area at the entrance to the Rotterdam Waterway

In addition to the usual suite of seabed mapping instrumentation, an ODIM Brooke Ocean MVP30 was temporarily installed on the aft deck of the RWS survey vessel *Corvus* for the duration of the trial. The MVP30 allows for acquisition of near vertical data profiles through the water column while underway and is ideally suited to sample sound speed profiles for hydrographic surveying (Furlong et al., 1997). Over the course of the seven day trial, 2,151 sound speed casts were acquired in several test survey areas and over long sections running from Maassluis to an area just offshore of the mouth of the Waterway (locations A and E in *Figure 9*, respectively). Given the estuarine nature of the trial location, it was important to understand the salinity variations throughout the water column, however, a CTD probe was unavailable at the time of the trial. As a substitute, an Applied Microsystems Limited (AML) sound speed and temperature probe was used such that salinity could be approximated by reverse calculation from the simultaneous sound speed and temperature measurements using the UNESCO standard equation for speed of sound in seawater (Fofonoff and Millard, 1983).
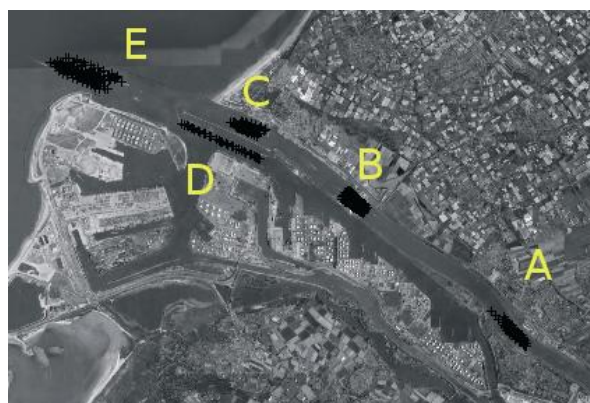
Figure 9: Satellite image indicating sound speed cast locations in Rotterdam Waterway, March 2009. Data courtesy of Rijkswaterstaat (Dutch Public Works). Cast locations are indicated for several survey areas as black crosses. Text labels correspond to plots in figures 14 through 19

Figure 10 provides an example of typical conditions as measured over a short section of the river whereas *Figures 11 through 13* depict the spatio-temporal variability of the conditions in the river channel over various stages of the tide for three days of the seven day trial. The observed temperature and salinity variations are consistent with a salt wedge type estuary with a strongly stratified water mass in which fast flowing surface river water is predominantly fresh and bottom water is predominantly salty with a pronounced pycnocline at the interface between the two layers. Salt water

intrudes upriver on the flood tide, acting like a wedge and sliding underneath the surface fresh water. During a falling tide, strong river currents rapidly flush the salty bottom water back to sea, forcing a retreat of the salt wedge, as seen in *Figure 12*. These types of environments are challenging to hydrographers as the majority of the variability is in the depth of the interface between the fresh and salt water, with the interfacial depth varying strongly in space and time (note the turbulent interface between the two layers in *Figure 11*). As the change in sound speed can be quite dramatic at the interface between the fresh and salt water, soundings can refract quite strongly leading to significant sounding uncertainty with seemingly small variations in the interfacial depth.
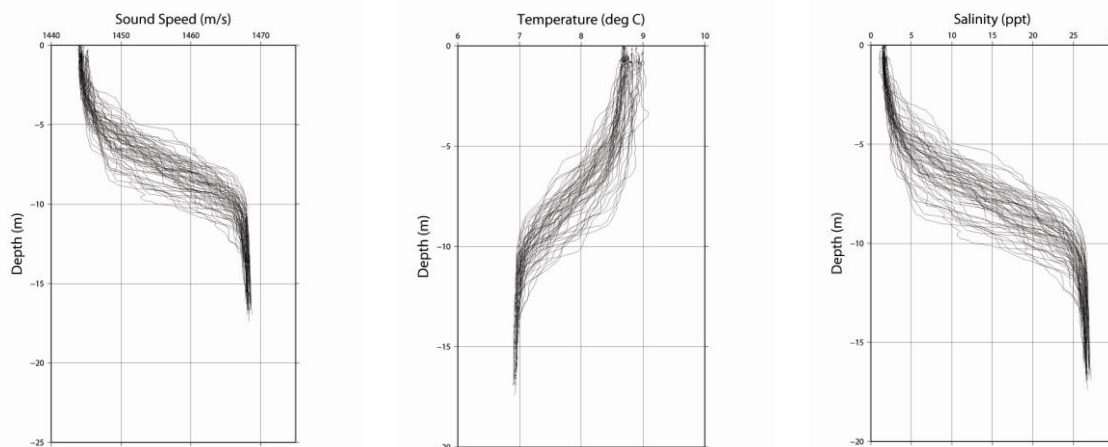
Figure 10: Sound speed, temperature and salinity profiles collected over a 1.5 hour period on a falling tide. The 60 casts were acquired in a 1.5 km long section of the waterway at location A in Figure 9. Sound speed, temperature and salinity are plotted from left to right. Recall that salinity was calculated from the sound speed and temperature measurements.
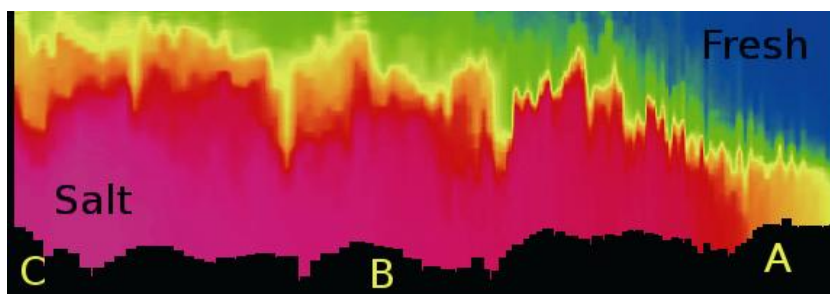
Figure 11: Vertical salinity section (20 m deep) over a distance of 11.5 km from station A to C, collected during high tide on March 25th.
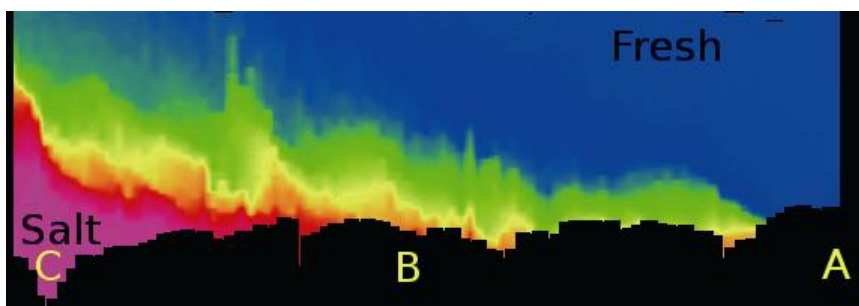
Figure 12: Vertical salinity section from station A to C, collected towards the end of a double low tide on March 30th
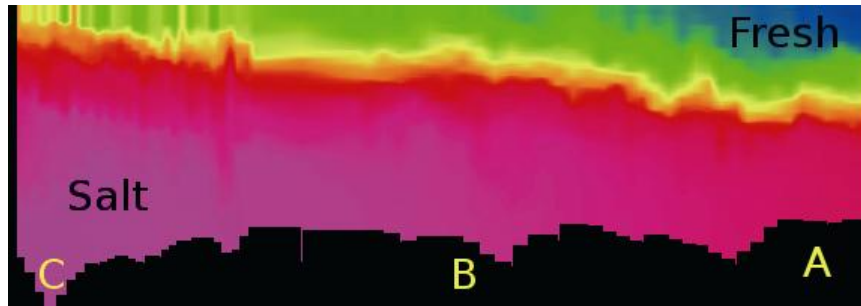
Figure 13: Vertical salinity section from station A to C, collected during a falling tide on April 2nd

3.2 Variability Analysis

In this section, we demonstrate how Variability Analysis (VA) can be used to quantify the spatial and temporal variations of a survey area's water column characteristics and how one might use this type of information in survey planning and execution. Plots of sound speed profiles and v-wedges derived from them are shown for locations A through E in *Figures 14* through 19, respectively. In each case, several tens of casts were acquired at each location (on different days) over the course of a few hours as the *Corvus* undertook typical survey operations at each location. This approach sampled the spatio-temporal variability of the water mass that the vessel would have had to contend with during routine survey operations, i.e. the casts do not represent a measure of the temporal variability at a fixed location.

Before proceeding with a discussion of the casts at each location, it is important to discuss a limitation of these analyses, that of ray tracing beyond the last observed sample in a sound speed profile. This is a problem that is common in hydrographic surveying ray tracing applications. Some software packages force the user to extend the cast to the required depth while others hold the last observed sound speed to the required ray tracing depth. As a false extension of a cast could bias our analyses, we have deliberately chosen to halt ray tracing beyond the terminal depth of each cast. Thus, the ray paths from shallower casts do not contribute at greater depths and the sample mean and standard deviation calculated in the analyses lock on to the potentially much tighter distribution of the deeper casts in each set. Unfortunately, this has the effect of introducing discontinuities in the various uncertainty wedge representations. In some cases, the discontinuities are easily remedied by extending all casts to the same depth, as is the case with the casts of location A *(Figure 14)*. In other cases it is unclear how casts should be extended, for example the casts from location B *(Figure 16)*. For our analyses, we focus on the uncertainties at the last depth prior to the first discontinuity, essentially limiting the investigation to the maximum depth that all casts achieved (i.e. the depth of the shallowest cast).
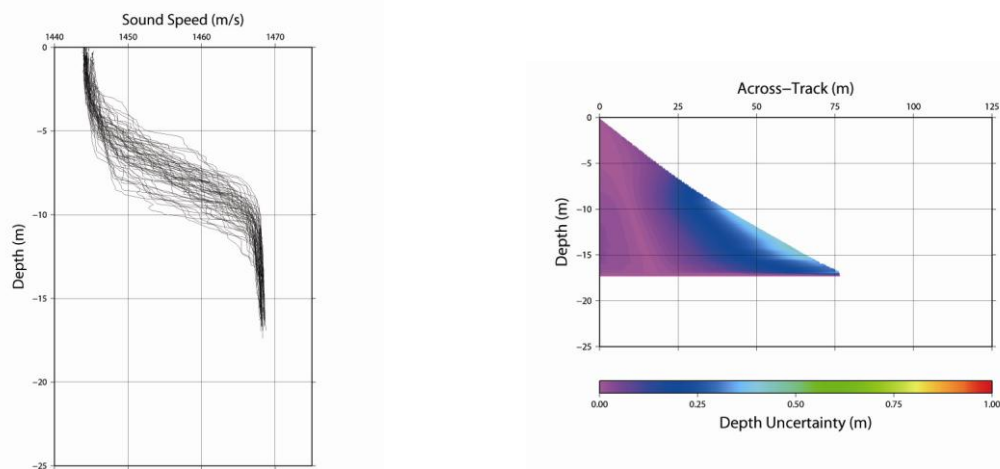
Figure 14: Sound speed casts and v-wedge for a 1.5 hour period near Maassluis in the Rotterdam Waterway (60 casts, location A in Figure 9).

Examining location A first, the mid-water interfacial depth varies vertically by nearly 5 m and introduces significant outer beam uncertainty below depths of 5 m. Referring to the salinity section in *Figure 12*, it is clear that there are stages of the tide where the salt water in the lower layer is flushed away at location A. Though the potential uncertainty quantified by the v-wedge is non-negligible for the stage of the tide over which the casts of location A were gathered, a patient surveyor might instead choose to wait for an appropriate stage of the tide before surveying in this area. That is, armed with nothing but a tide table and a conventional sound speed profiling instrument, the surveyor could collect exploratory casts up the river on a falling tide until the terminus of the salt wedge was found. Once found, a survey could proceed slightly upstream of the salt wedge with little concern for the troublesome variability associated with the wedge as it is safely downstream of the survey location and not likely to return until the tide begins to rise after low water.

Turning to location B, the variability in the pycnocline depth is more pronounced and dominates over a larger portion of the water column, perhaps half of the water column as opposed to one third as was observed at location A. Arguably, this is partially explained by the longer sampling period at location B: the VA is exposed to more of the falling tide, increasing the perceived effect of variability. Location B, however, was characterized by significant spatial along-track variability in the pycnocline depth relative to location A, with the depth of the pycnocline falling by roughly 5 m over the course of a survey line with pronounced short period oscillations of 1-2 m superimposed. *Figure 15* demonstrates the marked difference in along track variability between location A and B by plotting the depth of the 11 ppt isohaline against elapsed survey time, with each segment corresponding to observations made over a single survey line.
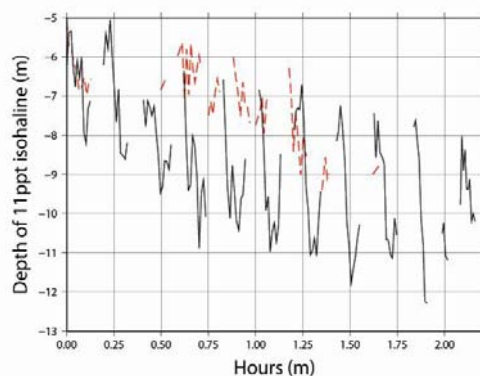
Figure 15: Variation in the depth of the 11 ppt isohaline surface plotted against hours since start of survey at locations A and B (dashed red and solid black lines, respectively). When referring to figures 14 and 16, the 11 ppt isohaline loosely corresponds to a sound speed of 1453 m s^{-1}
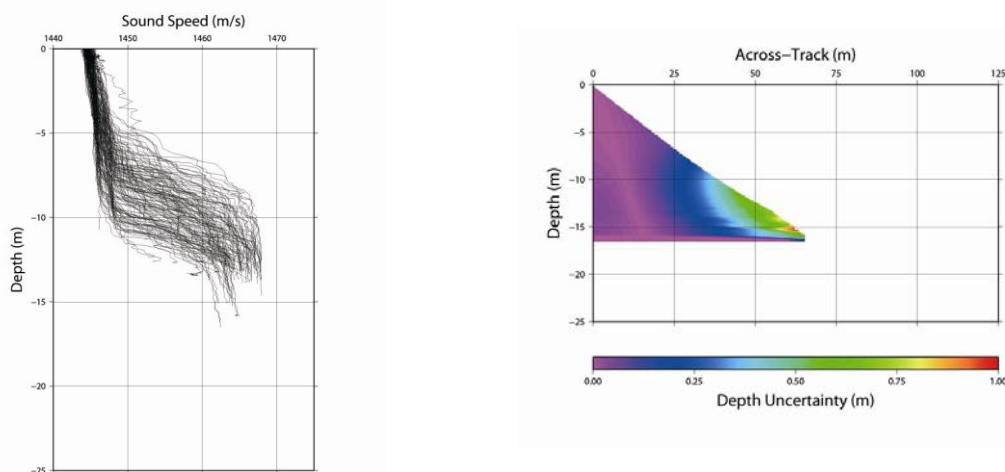
Figure 16: Sound speed casts and v-wedge for a 2.5 hour period while surveying within the surge barrier structure of the Rotterdam Waterway (148 casts, location B in Figure 9)

There are stages of the tide where the variability is much lower in the water column, for example, compare the halocline depth at location B in *Figure 11* and *Figure 12*. Though none of the salinity sections in *Figures 11 through 13* show location B being completely free of the effects of the migrating salt wedge, other observed sections show an occasional near retreat of the salt wedge as far as location B, thus there is the potential to work around the tide at this location as well. Even if the salt wedge does not retreat completely downstream of location B, it is advantageous to have the variability constrained to deeper depths. Location C *(Figure 17)* provides an example of the advantages of such a near retreat: at this location the variability associated with the interface between salt and fresh water was observed to occur much deeper in the water column as compared to locations A and B. As a result, the potential uncertainty is substantially lower when compared to the VA results for locations A and B.

The Caland Canal section of the Waterway (location D, *Figure 18)* is cut off from upstream freshwater inflow from the river, thus surveys in this area are less likely to suffer from the refraction problems that come with working in the main channel of the Waterway though it is possible that brackish surface layer water is forced upstream during a rising tide (the area was only sampled at low tide). In this area, it is perhaps possible to sample the water column once every few hours and still maintain accuracy. This type of information is useful for survey vessel fleet management. For example, one might assign this site to a vessel equipped with static profiling systems and reserve vessels equipped with underway profiling systems for the main river channel where variability is more of a problem.

Figure 17: Sound speed casts and v-wedge for a 1.0 hour period at the entrance to the Rotterdam Waterway
(52 casts, location C in Figure 9)
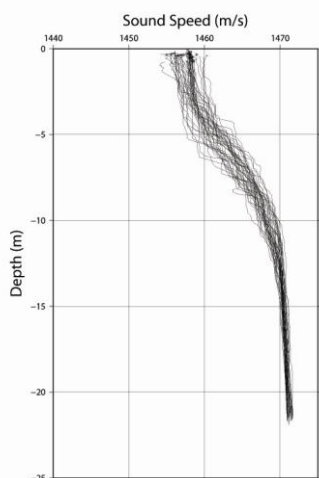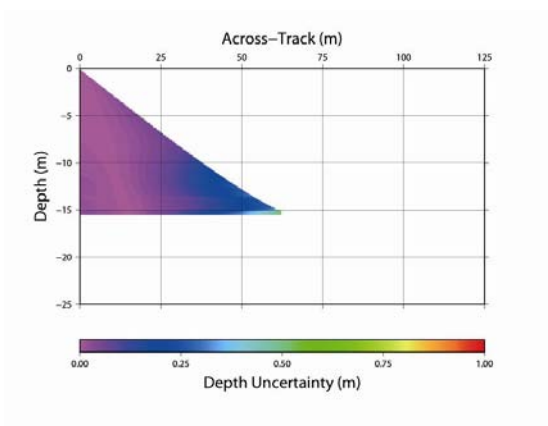
Figure 18: Sound speed casts and v-wedge for a 2.5 hour period in the Caland Canal portion of the Rotterdam Waterway (44 casts, location D in Figure 9)
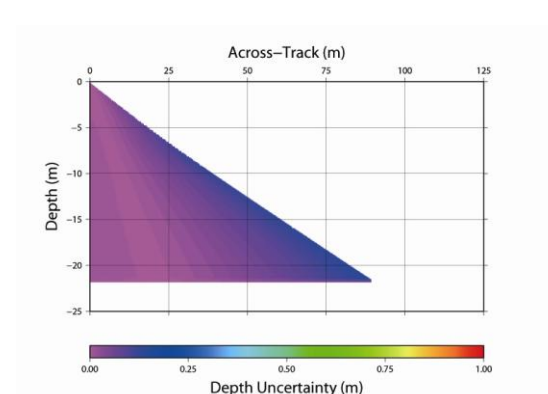
At the mouth of the river (location E), the outflow of the river was limited to a thin surface layer *(Figure 19)*. As the variability occurs in the upper part of the water column, the divergence of ray paths occurs early on during ray tracing, introducing sounding uncertainty that persists over the remainder of the ray path. In this area, RWS often use a deep draft vessel to counteract the surface variability, however, the v-wedges of *Figures 20 and 21* demonstrate that it is far more important to have a surface sound speed probe than to have a deep draft. Though a v-wedge is a convenient representation format for visualization and look-up of uncertainty, it is not well suited for intercomparison. For comparison purposes, the data from one depth (24 m) is extracted across the swath from each of the v-wedges and plotted in *Figure 22*, allowing for a more useful examination of the potential uncertainty for the four possible combinations of draft and surface sound speed probe. In this format, it is clear that the VA results support the idea that a deep draft vessel suffers less from the surface variability. Indeed, the probe-aided, deep draft vessel is the only case where the entire angular sector falls within the 0.75% water depth alloted towards sources of uncertainty that grow with depth (though it absorbs all of the allowable

uncertainty, leaving no room for other sources of uncertainty such as roll) (International Hydrographic Organization, 2008). The allowable vertical uncertainties for the RWS survey orders and IHO special order are included in the plot for context (RWS order A allows 0.10 m + 0.75% water depth uncertainty whereas order B allows for 0.15 m + 0.75% water depth).

An opposite effect occurs when using a deep draft vessel in which the transducer's draft places it in the variable layer, e.g. a 4 m draft vessel at location A. Examining the uncertainty across the swath at a single depth, *Figure 23* shows that the surveyor would be doubly penalized for using a deep draft vessel: firstly from the increase in uncertainty, and secondly from the loss of swath width. The first effect is perhaps non-intuitive but has a simple explanation. As the draft of the vessel increases, any given spot on the seafloor is sounded with an ever increasing incidence angle; the cost of increasing the obliquity of a sounding is an increase in uncertainty due to refraction. Deep draft vessels are thus not a panacea and should be limited to areas where surface variability is the predominant source of refraction based uncertainty.
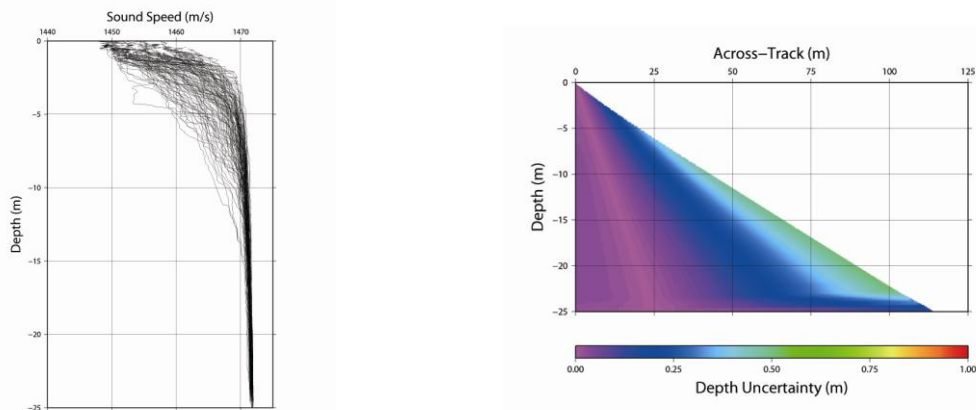
Figure 19: Sound speed casts and v-wedge for a 2.5 hour period just off the entrance to the Rotterdam Waterway (106 casts, location E in Figure 9).
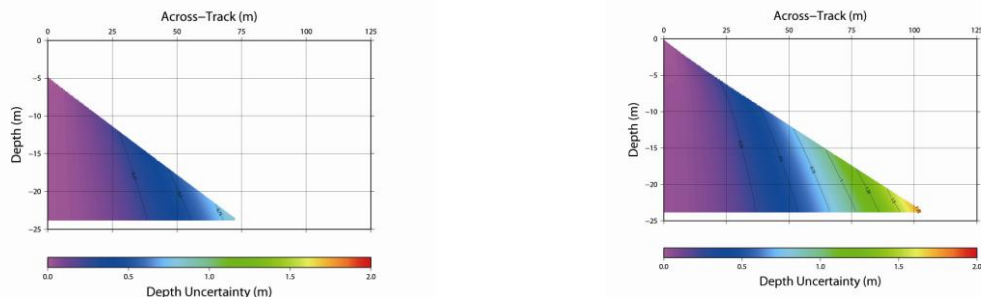
Figure 20: Variability wedges computed for a deep (4.0 m) and shallow (0.3 m) draft vessel without a surface sound speed probe for the casts acquired in Location E in Figure 9.
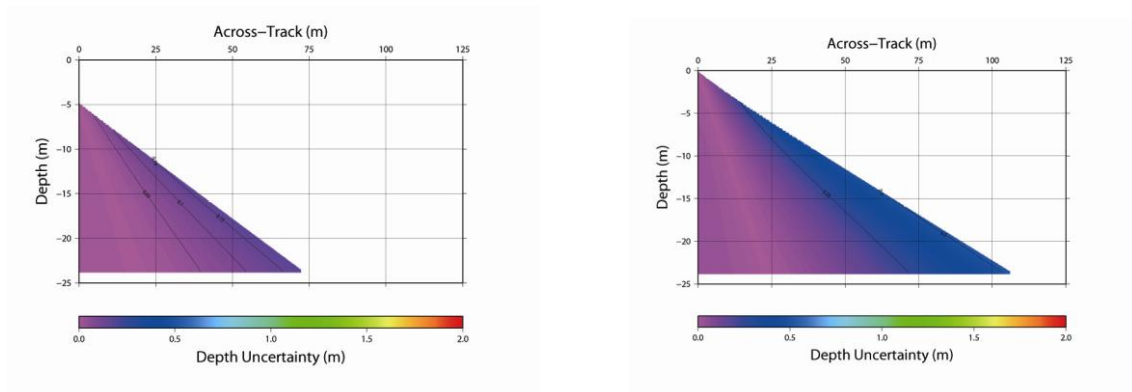
Figure 21: Variability wedges computed for a deep and shallow draft vessel with a surface sound speed probe for the casts acquired in Location E in Figure 9. Compare with variability wedges of Figure 20
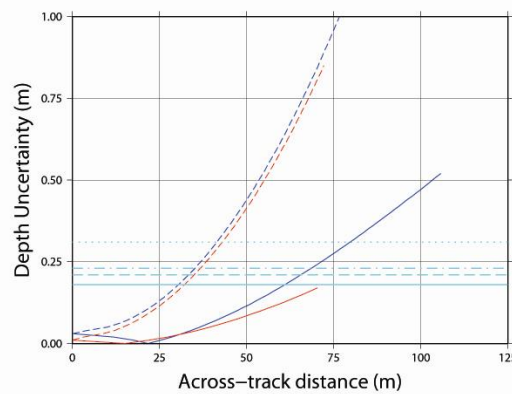
Figure 22: Vertical uncertainty at 24 m depth for deep draft (red) and shallow draft (blue). Solid and dashed lines represent VA results with and without a sound speed probe, respectively. Allowable vertical uncertainties of RWS survey orders are plotted in cyan using the following convention: solid = 0.75% water depth, dashed = RWS Order A, dashed and dots = RWS Order B, dots = IHO Special Order. This convention is followed throughout the remainder of this work
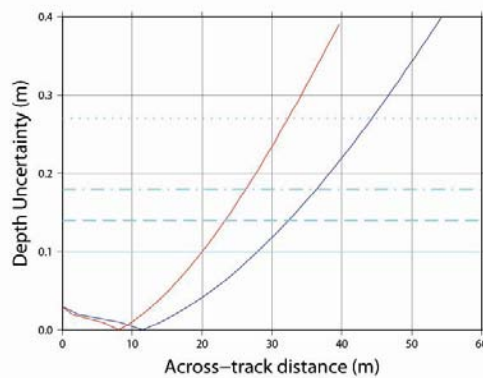
Figure 23: Depth uncertainty at 13 m of depth at location A, with simulated drafts of 0.3 m (blue) and 4.0 m (red)

We conclude this section by summarizing the VA for the five locations by presenting the potential uncertainty across the swath at a depth of 13 m in *Figure 24*. Recall that a VA quantifies the potential uncertainty for a set of measured conditions. Of all the locations, perhaps D is the "easiest" to survey in that it presents the least challenging conditions. All other areas are subject, at some stage of the tide, to significant variability that limits the effectiveness of the wide angular sector systems favoured by RWS. The uncertainty of the outer portion of the swath for all locations except D significantly exceeds 0.75% water depth. If we conservatively allot one third of the 0.75% to refraction, i.e. 0.25%, and leave the remaining 0.5% for other sources of depth dependant uncertainty, then the maximum horizontal distance from the sounder that would remain within tolerable limits of uncertainty is reduced to slightly less than 25 m for locations A, C and E and approximately 15 m for location B, giving swath widths of 50 m and 30 m, respectively. Even though the Kongsberg EM3002D MBES onboard the *Corvus* is capable of an angular sector of 150°, these environments are far too variable to permit such a wide sector when one has a limited ability to sample the water column.
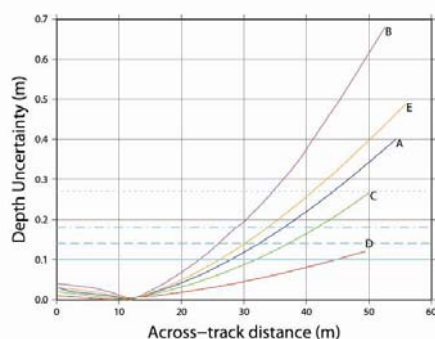
Figure 24: Depth uncertainty at 13 m of depth due to water mass variability for locations A through E

3.3 Uncertainty Wedge Analysis

In this section we demonstrate how UWA can quantify the uncertainty as a function of how the water mass is sampled, the aim being to understand whether or not underway sampling technology such as the MVP can improve uncertainty and survey efficiency. Location B is chosen as an example as it proved to be the most dynamic area observed, based on the VA for that location and stage of tide.

Sets of b-wedges were computed for the entire set of casts with each cast in a survey line being compared to its predecessor; this provides an estimate of the bias suffered immediately before the collection of the cast. An s-wedge was computed to summarize the standard deviation associated with use of the full set of casts from the MVP. Two sub-sampling analyses were performed in which the full set was used to gauge the impact of other sampling schemes. In these cases, the full set was thinned to match simulated sampling intervals of 160 seconds and 30 minutes (the MVP sampled every 40 seconds). B-wedges were computed by comparing the casts in the thinned set to the casts in the full set, e.g. if 9 casts were collected and casts 1, 4 and 7 were the casts from the simulated set, then b-wedges were computed for the following pairs: {1,2}, {1,3}, {1,4}, {4,5}, {4,6}, {4,7}, {7,8} and {7,9}. These b-wedges were compiled into an s-wedge, horizontal sections of which are shown in *Figure 25,* along with the estimated uncertainty from the VA and the MVP s-wedge. Not surprisingly, all sampling scenarios improve upon the potential uncertainty and higher sampling rates yield better control over sounding uncertainty. On the other hand, despite the MVP sampling as often as physically possible, there is still appreciable uncertainty in the outermost swath portions of the swath. Aiming again to maintain uncertainty below 0.25% of water depth, the maximum across-track distance within specification is reduced to 20 m, giving a swath width of roughly 40 m.
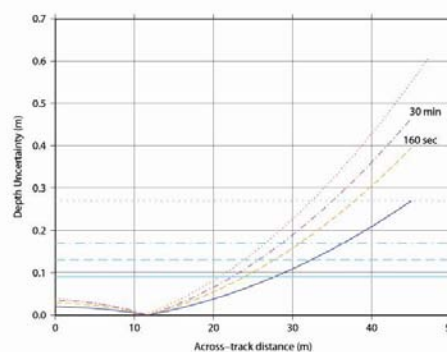
Figure 25: UWA and VA results from location B for a depth of 12 m. The dotted red line represents the potential uncertainty as predicted by the VA whereas the blue indicates the uncertainty associated with maximum use of the MVP system, i.e. the best case scenario (sampling roughly every 40 seconds). The entire MVP dataset is used to simulate the impact of sampling every 30 minutes (magenta dashes and dots) and every 160 seconds (orange dashes)

Turning back to the salinity sections of *Figures 11 through 13*, some insight into the underlying problem can be gleaned through a UWA of the three transects. As before, b-wedges were computed and compiled into an s-wedge for each transect. The depth uncertainty at a depth of 13 m is extracted from the s-wedges and is plotted for all three transects in *Figure 26*; it is clear that conditions in transect 1 are much more challenging, on average. Interesting details can be masked in the compilation of an s-wedge, however, and it is often beneficial to examine the b-wedges in some manner, however, it is difficult to examine several hundred images for comparative purposes. In this case, the bias of the outermost beam (at a depth of 13 m), is plotted against distance from location C in *Figure 27*, allowing for inter-comparison. Examining the uppermost panel of Figure, that associated with *Figure 11*, the largest bias occurs in the turbulent front between salt water and fresh water on a rising tide (high tide at location A lags that at the mouth by about one hour); when appreciable biases occur at such a high rate, it indicates that the last cast serves as a poor predictor for the next and the environment is far too variable to work in, even with an underway profiler. Compared to the bias signal of the first section, those of the other two sections seems benign though significant bias events were observed. These transects indicate that, under certain tidal conditions, an underway profiling system enables acquisition of survey lines several kilometers long (as compared to the usual 1 km box surveys), however, one must take care to avoid the front of the rising tide. All hope is not lost on the first section. Just as it is possible to chase the retreating salt wedge out to sea at location A, it would be equally plausible to follow the salt wedge as it intrudes up the river, as can be seen from the western 5 km section of the upper panel in *Figure 27*, though this might best be performed with a deeper draft vessel (refer to the orange dashed line in the upper panel of *Figure 27)*.
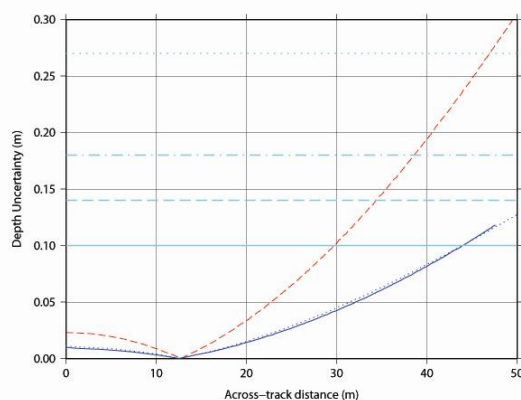
Figure 26: UWA results for 13 m depth from the three longitudinal sections of figures 11, 12 and 13 (red dashed, solid blue, dotted blue)
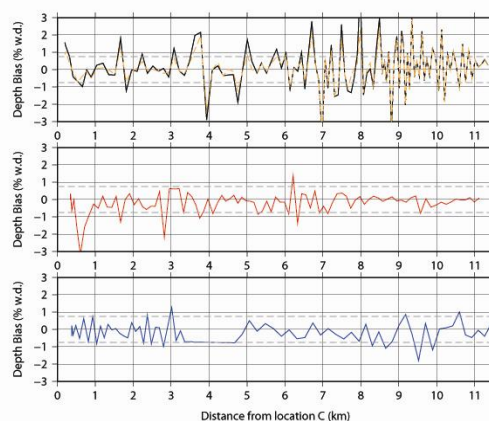
Figure 27: Outer beam bias at a depth of 13 m from sequential b-wedges from the three longitudinal sections of figures 11, 12 and 13 (top to bottom, respectively). The black solid and orange dashed lines in the upper panel compare use of a shallow and deep draft transducer. Grey dashed lines indicate +/- 0.75% water depth

4. Integration into CUBE

CUBE (Calder and Mayer, 2003) is a computer-assisted hydrography algorithm that attempts to estimate the true depth at any given position within the survey area, and provide some guidance to the user as to how well that depth is known; CUBE is an acronym for "Combined Uncertainty and Bathymetry Estimator". The essence of the CUBE algorithm is the understanding, modeling and utilisation of the uncertainty of the measurements that go into the depth soundings that are collected by MBES equipment; for dense MBES data, CUBE can provide very rapid, robust depth estimates from raw data and assist the user in assessing which data needs attention, improving the data workflow.

While CUBE itself does not mandate how uncertainties are computed for the soundings that it ingests, it does require that the uncertainties are "reasonable" in the sense that they need to reflect at least a first-order accurate depiction of the actual variability of the soundings for the algorithm to operate as intended. Integration of the current work into CUBE therefore requires that we address the problem of how to integrate the uncertainty due to sound speed profile (SSP) spatio-temporal effects into the computation of the total propagated uncertainty (TPU), and consider the implications that this has for CUBE's operation.

During development of the algorithm, the Hare-Godin-Mayer (Hare et al., 1995) model was used to construct TPU estimates for the soundings, and although the model has been refined since, it is still the most commonly used model for TPU estimation in current use. In this model, the effects of sound speed uncertainty are contained in terms that affect the fundamental uncertainties of range and angle estimation. Due to the paucity of information about the degree of spatio-temporal uncertainty at the time, however, the effects of measurement uncertainty in the SSP and the spatio-temporal variability of the water mass as reflected in the profile were combined into a single uncertainty term resulting in a simpler computational model, but a cruder representation of the true effects of the oceanographic environment. In particular, in environments where there is significant spatial specificity to the degree of SSP variation, the model is forced to adopt a pessimistic uncertainty analysis in order to cover the worst-case areas, and provides little assistance in assessing the effects for the user. This also results in reduction of processing power in CUBE since much of the algorithm's ability to determine likely depth reconstructions (which is essential to the efficiency of the algorithm) is predicated on the uncertainty reflecting the true nature of the soundings. By adopting a pessimistic analysis, the robustness of the estimation is weakened everywhere.

We now have the opportunity to refine this model through use of the UWA to reflect the spatio-temporal uncertainty. The current model represents the depth of the sounding by

$$d = r\cos(\theta + \rho)\cos\varphi = r\cos(\theta')\cos\varphi \qquad (1)$$

with indicated range r and angle θ, roll ρ and pitch φ. (In the following, we work with the combined angle θ' for simplicity of presentation.) Using the principle of propagation of uncertainty, the predicted uncertainty in depth is

$$\sigma_d^2 = \left(\frac{\partial d}{\partial r}\right)^2 \sigma_r^2 + \left(\frac{\partial d}{\partial \theta'}\right)^2 \sigma_{\theta'}^2 + \left(\frac{\partial d}{\partial \varphi}\right)^2 \sigma_\varphi^2 \qquad (2)$$

Pitch and roll are unaffected by SSP effects, but if we trace the effects due to range and angle uncertainty through the vertical model, we find that they are, respectively

$$\sigma_{d(r)}^2 = \cos^2\varphi\cos^2\theta'\sigma_r^2 \qquad (3)$$

$$\sigma_{d(\theta)}^2 = r^2\sin^2\theta'\cos^2\varphi\sigma_\theta^2 \qquad (4)$$

and that the effects of the various components of uncertainty in range and angle are linear once multiplied by their respective sensitivity factors (ISO, 1995). Knowing that Hare et al. (1995) show that the uncertainty of range and angle measurement associated with SSP effects can be approximated as

$$\sigma_{r(SSP)}^2 = \left(\frac{r}{v}\right)^2 \sigma_{v(SSP)}^2 \qquad (5)$$

$$\sigma_{\theta(SSP)}^2 = \left(\frac{\tan\theta'}{2v}\right)^2 \sigma_{v(SSP)}^2 \qquad (6)$$

respectively, we can refactor (3) and (4) to extract the SSP specific terms, and evaluate the remainder of the model as at present. Specifically, if we assume that

$$\sigma_{v(SSP)}^2 = \sigma_{v(SSP-M)}^2 + \sigma_{v(SSP-ST)}^2 \qquad (7)$$

for measurement and spatio-temporal effects respectively, we can substitute in (5) and (6), extract the spatio-temporal component and develop a modified formulation that replaces the SSP spatio-temporal terms with the output of the UWA look-up tables, neglecting the terms

$$\sigma_{d(SSP)}^2 = \frac{1}{4}\left(\cos^4\theta' + \sin^4\theta'\frac{r^2\cos^2\varphi}{v^2\cos^2\theta'}\right)\sigma_{v(SSP-ST)}^2 \qquad (8)$$

in the vertical and

$$\sigma_{p(SSP)}^2 = \left(\frac{r}{v}\right)^2 \sigma_{v(SSP-ST)}^2 \times \left[\left(\cos\theta'\cos\varphi\right)^2 + \frac{1}{4}\left(\sin\theta'\cos\varphi\right)^2\tan^2\theta'\right] \qquad (9)$$

in the horizontal from the original model. In practice, this can be done simply by setting the value of $\sigma^2_{v(SSP)}$ used at present to represent only the measurement uncertainty of the SSP component, and then adding the UWA-derived look-up table values in vertical and horizontal to the output of the current model.

There are three main implications for this technique applied to the CUBE algorithm. First, allowing the TPU algorithm to properly reflect the uncertainty of the SSP in the individual soundings should greatly assist the CUBE algorithm in maintaining robustness throughout the survey area. A great deal of the power of the CUBE algorithm resides in its ability to automatically separate groups of soundings that are mutually inconsistent, and this action relies on the uncertainties of the soundings reflecting the variability expected in them. With empirical estimates of uncertainty applied, the number of stray soundings that are incorporated into a internally consistent group should decrease, which will lead to better in-group depth estimates, and therefore less interaction on the part of the user.

Secondly (and an immediate corollary of the first implication), in areas where there are significant SSP spatio-temporal effects, the increase in uncertainty applied in the UWA encourages the algorithm to consider soundings that are refracted as "sufficiently similar" that they can be accommodated as one consistent group, therefore reducing the number of spurious secondary hypotheses on the actual depth that are formed. Reduction of the number of hypotheses that are formed makes it simpler for the algorithm to assess which is most likely, and improves the algorithm's ability to choose the "right" hypothesis to report to the user. The efficiency with which the user can process data depends strongly on how often the algorithm can do this, so the improved uncertainty estimates should reduce operator time correspondingly.

Thirdly, the uncertainty that is assessed within the group of soundings that are combined to make the depth estimate reported to the user as the primary hypothesis will, under the proposed scheme, better reflect the actual uncertainty in the data. At present, if the soundings have higher uncertainty than predicted (e.g., due to refraction), the algorithm tends to make secondary hypotheses. The choice of which assessment of uncertainty to

report to the user from the CUBE algorithm has been subject to some debate, but is currently most often an estimate of the standard deviation of the soundings used to compute the hypothesis. Currently, therefore, the assessment within the secondary hypotheses will only reflect the uncertainty of one group of soundings in the area, typically those from one pass of the MBES, and therefore under-estimates the actual uncertainty of the data in the area. In the proposed scheme, the increased uncertainty associated with the SSP spatio-temporal effects would cause soundings with higher refraction effects to be considered as one hypothesis (per the previous implication), and therefore the uncertainty reported to the user would be correspondingly higher. This more accurately quantifies the actual uncertainty of the data in the area, and should result in better modeling and assessment of the value of the data in the area for the surveyors and the end users. Note that this is not to say that the data is necessarily useless under these conditions: depending on the survey standards in effect, the surveyor might assess the data as adequate, even given the increased uncertainty reflected in the final output. The outputs of the algorithm will, however, better reflect reality.

5.   Conclusion

Oceanographic pre-analysis campaigns can be undertaken in areas where repetitive, high accuracy, surveys are the norm for safety of navigation. The analysis techniques presented herein allow the hydrographic surveyor to process oceanographic data into information; insights gained during such an exercise can help direct immediate or future field operations. As the uncertainty wedge representation provides objective and realistic estimates of uncertainty for each sounding based on observed water column conditions, it has the potential to augment the fidelity of the water column variability component of uncertainty models used in the hydrographic community.

6.   Future Work

The sample analyses presented herein are not meant to be exhaustive and further investigation is warranted to determine how these findings would change with variations in tides, weather patterns and seasons. Further sampling and/or research is required to address remaining issues such as these.

VA and UWA rely heavily on having an oversampled water mass, something which is not always practical to collect. Occasionally one may have access to historic data or data from hydrodynamic circulation models. Future work will investigate whether UWA and VA give reasonable results when given (a) much smaller data sets of casts, and (b) predicted casts from oceanographic models.

7. Acknowledgements

This work was supported by the ArcticNet NCE, sponsors of the OMG and by NOAA under grant NA05NOS4001153. The authors would like to thank Rijkswaterstaat for the opportunity to participate in the Rotterdam Waterway trial as it provided the perfect data set for which to showcase the analysis methods presented in this work.

8. References

Beaudoin, J.D., Hughes Clarke, J.E. and J. Bartlett (2004). Application of surface sound speed measurements in postprocessing for multi-sector multibeam echosounders. International Hydrographic Review, 5(3), 2004.

Beaudoin, J.D. (2008). Real-time monitoring of uncertainty due to refraction in multibeam echosounding. In Proc. Shallow Survey 2008, Oct 2008.

Calder, B.R. and L. A. Mayer (2003). Automatic processing of high-rate, high-density multibeam echosounder data. Geochem., Geophys. and Geosystems (G3) DID 10.1029/2002GC000486, 4(6).

Calder, B., Kraft, B., de Moustier, C., Lewis, J. and P. Stein (2004). Model-based refraction correction in intermediate depth multibeam echosounder survey. In Proc., European Conference on Underwater Acoustics, 2004.

Cartwright, D.S. and J. E. Hughes Clarke (2002). Multibeam surveys of the Frazer river delta, coping with an extreme refraction environment. In Proc. Canadian Hydrographic Conference, May 2002.

Fofonoff, N.P. and R. C. Millard Jr. (1983). Algorithms for computation of fundamental properties of seawater. Technical Report 44, Division of Marine Sciences, UNESCO.

Furlong, A., Beanlands, B. and M. Chin-Yee (1997). Moving vessel profiler (MVP) real time near vertical data profiles at 12 knots. In Proc. IEEE Oceans 1997, volume 1, pages 229–234. IEEE, Oct 1997.

Hare, R., Godin, A. and L.A. Mayer (1995). Accuracy estimation of Canadian swath (multibeam) and sweep (multitransducer) sounding systems. Technical report, Canadian Hydrographic Service.

Hughes Clarke, J.E., Lamplugh, M. and E. Kammerer (2000). Integration of near-continuous sound speed profile information. In Proc. Canadian Hydrographic Conference, Montreal, QC, Canada, 2000.

International Hydrographic Organization (2008). IHO standards for hydrographic surveys, special publication no. 44, 5th edition. Technical report, IHO, Monaco

International Organization for Standardization (1995). Guide to the expression of uncertainty in measurements. Technical report, ISO, Geneva. ISBN 92-67-10188-9.

Kongsberg Maritime AS (2006). Operators Manual - EM Series Datagram Format (20-01-06).

Medwin, H. and C. S. Clay (1998). *Fundamentals of Acoustical Oceanography*. Academic Press.

Appendix A

Simulation of Surface Sound Speed Probe

A surface sound speed probe is often required to ensure correct electronic beam steering angles with linear transducer arrays. It is also often used to augment the sound speed profile during ray tracing by (1) using the measured surface value as "the initial entry in the sound speed profile used in the ray tracing calculations" (Kongsberg Maritime AS, 2006) or (2) calculating Snell's constant, or the ray parameter, with the observed surface value prior to ray tracing (Beaudoin et al., 2004). As pointed out by Cartwright and Hughes Clarke (2002), the incorporation of the surface sound speed measurement has a significant effect on the behaviour of a ray tracing algorithm; in some cases it allows for a graceful recovery from surface layer variability as long as the deeper portion of the water mass is relatively invariant.

Regardless of this potential gain, the inclusion of the surface sound speed as an additional measurement fundamentally changes the behaviour of a ray tracing algorithm, thus its effect on ray tracing should be included in uncertainty models.

For UWA, we mimic the use of a surface sound speed probe by retrieving the sound speed at transducer depth from the reference profile and using this to compute the ray parameter for the test cast ray trace without modifying the test cast. One must take care, however, to only perform this additional step if the acquisition and/or post-processing software can accommodate the surface sound speed as an additional aiding measurement during sounding reduction, specifically the ray tracing portion of the procedure.

VA is based upon examining the divergence of several ray paths, with each ray path tied to a different sound speed profile. For a given travel time, depression angle and surface sound speed, the bundle of rays will land at some location in the potential sounding space. The scatter of their solutions about their mean position in the potential sounding space serves as an indicator of the sensitivity to water column variability. The problem is that we need to simulate the use of a common surface sound speed measurement as the initial entry into the water column during the ray trace for each ray in the bundle, but which sound speed should be used? It turns out that it does not matter.

Consider a ray trace with a depression angle of 20° (incidence angle of 70°) and sound speed of 1445 ms^{-1}. The ray parameter used in the ray trace is calculated as:

$$k_1 = \sin(70°)/1445$$

As the ray parameter is a function of depression angle and sound speed, there exists other angle/sound speed pairs that would yield the same ray parameter. For example, consider a surface sound speed of 1440 ms^{-1}. Snell's law is applied to determine which angle would give the same ray parameter:

$$k_2 = \sin(\theta)/1440 = k_1$$
$$\theta = \arcsin(1440\sin(70°)/1445) \approx 69.462°$$
$$\therefore \psi = 90° - \theta \approx 20.538°$$

where ψ is the depression angle.

If one were to perform an acoustic ray trace with a common sound speed profile and differing surface sound speed/depression angle pairs, the rays would share the exact same ray path, despite having different depression angles and different surface sound speeds. In essence, it is possible to get to the same location on the seafloor through a different launch angle and surface sound speed combination.

How does this apply to the simulation of the use of a surface sound speed probe in VA? If the above exercise is true for one ray, then it is true for all rays in a bundle of rays being investigated in a VA. One can arrive at the mean location by investigating a given depression angle and surface sound speed from one of the casts, or by using a different depression angle and a different surface sound speed, chosen from a different cast in the set. As all of the rays in the bundle will all arrive at their same respective positions in either case, then their relative positions with respect to their mean position will remain the same. It follows that the dispersion of the solutions about the mean location would also remain the same regardless of how the bundle of rays arrived at the mean location. In other words, any one of the casts can be chosen as a measurement of truth and we would eventually, through some combination of surface sound speed and depression angle, arrive at the same mean location and witness the same dispersion of the ray traced solutions. So, an arbitrary surface sound speed value could be chosen, and with a systematic sweep across the angular sector we will have visited every spot in the potential sounding space and calculated the dispersion in the same manner had another surface sound speed been chosen.

Note that the exact matching of ray traced solutions depends heavily on how the ray trace algorithm uses the additional surface sound speed measurement to augment the sound speed profile. The following procedure is used with the UNB method: (1) the surface sound speed and depression angle are used to define the ray parameter, and (2) the ray is immediately refracted at the beginning of the ray trace as if an infinitesimally thin layer of water exists at the transducer face in which the speed of sound is the measured surface sound speed. Deviation from this methodology will result in small discrepancies in the equality of the ray solutions when one modifies the surface speed or depression angle as we have in this exercise. For

example, simply replacing the sound speed at the transducer depth in the water column can yield slight inconsistencies in the results.

Biographies

Jonathan Beaudoin is a PhD student studying with the Ocean Mapping Group (OMG) at the University of New Brunswick in Fredericton, New Brunswick. His main research interest is the application of oceanographic databases for multibeam surveying. Jonathan is also a research assistant for the ArcticNet project, which sees him involved in all stages of ArcticNet mapping operations in the Canadian Arctic. He holds bachelor degrees in Geomatics Engineering and Computer Science, both from UNB.

Dr. Brian Calder (brc@ccom.unh.edu) is a Research Assistant Professor at the Center for Coastal and Ocean Mapping & Joint Hydrographic Center at the University of New Hampshire. He graduated MEng and PhD in Electrical & Electronic Engineering from Heriot-Watt University in Edinburgh, Scotland in 1994 and 1997 respectively, but was subsequently seduced into sonar signal processing for reasons that are now obscure. His research interests have previously covered speech recognition, texture

analysis, object detection in sidescan sonar, high-resolution sub-bottom profiling, simulation of forward-looking passive infrared images, acoustic modeling and pebble counting. Currently, they revolve around the application of statistical models to the problem of hydrographic data processing.

James Hiebert is a Physical Scientist in NOAA's Coast Survey Development Lab and has a background in Computer Science. He earned his M.S. from the University of Oregon in CS with foci in peer-to-peer networking and Internet routing. Most of James's free time is devoted to hiking, climbing, camping, running and generally exploring wild places.

Gretchen Imahori is a Physical Scientist/Lead Management and Program Analyst in NOAA's Office of Coast Survey and has a B.Sc. in Chemistry and a M.Sc. in Earth Sciences with a focus in Ocean Mapping. Since 1999, she has been employed by NOAA and working in different areas of Coast Survey ranging from hydrographic operations, technical writing and contract oversight to project management of the Hydrographic Services Review Panel (FACA), strategic planning and budget development.

Back to Contents